The work progress in 2025 with respect to the project objectives

O1. 1) Investigations of defects in n type 4H-SiC grown in different conditions (C/Si ratio, Nitrogen flow, growth rate) induced by irradiation with 6 MeV electrons, fluences up to $6x10^{14}/cm^2$; 2) thermal stability studies aimed to bring evidence for chemical identity of $Z_{1,2}$ and $EH_{6,7}$ centers; 3) As-grown samples provided by DRD3 or by NIMP were also investigated, especially for following the correlation between $Z_{1,2}$ and $EH_{6,7}$.

O2. 1) electrical investigations (resistivity, Hall, CV/IV, DLTS) on Si diodes mimicking the gain layer in LGADs (DRD3 project in WP3), fabricated with different flavours of B, C, O and P impurities (see Fig. 1). This type of diodes is labelled in the following as GL diodes. For each flavour, one diode with and one without C (only $5x10^{13}$ C/cm^2) have been characterized prior and after 23 GeV protons irradiation and few steps of subsecvent annealing at 60ºC; 2) FTIR structural investigations in irradiated samples at ambient temperatures (we encountered problems with the recently aquired low temperature FTIR module); 3) defect investigations and annealing studies in nLGADs exposed to local ion beam irradiation with low-penetrating 1.285 MeV gallium ions, p-type LGADs exposed to low-energy X-ray photons (around 2 keV) and deep-LGADs with and without C-implantation at the request of DRD3 collaborators (CNM Barcelona and PSI).

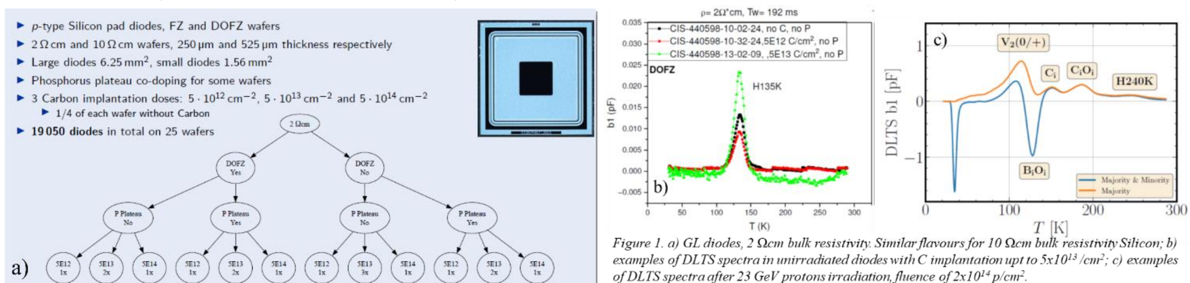

Figure 1. a) GL diodes, 2 Ωcm bulk resistivity. Similar flavours for 10 Ωcm bulk resistivity Silicon; b) examples of DLTS spectra in unirradiated diodes with C implantation upt to $5x10^{13}$ $/cm^2$; c) examples of DLTS spectra after 23 GeV protons irradiation, fluence of $2x10^{14}$ p/cm^2.

O3. 1) Geant4 simulations have been performed to simulate the effects of 1 MeV neutron and 23GeV proton irradiation in n++/p+ junctions; The NIEL has been determined for the different regions of the junctions; 2) Molecular dynamics (MD) simulations using the LAMMPS code on bulk silicon structures, showing the generation of vacancy-interstitial (V-I) pairs and the evolution of the complex defects in time, in canonical conditions; 3) Investigation of neutral and charged point defects in the framework of *ab initio* density functional theory (DFT) calculations using the SIESTA package; A high throughput workflow has been implemented to determine possible metastable states and the formation energies of several defects, with a particular focus on donor-type defects (e.g. $B_{Si}Si_i$, B_iO_i, C_iO_i).

The gain in expertise (scientific and technological) in 2025

On SiC: *Defect spectroscopies performed on as-grown samples and after irradiation with 6 MeV electrons followed by annealing experiments brought evidences for establishing the nature and introduction rates of radiation induced defects in relation with the growth conditions of 4H-SiC.* Especially the generation of $Z_{1,2}$ and $EH_{6,7}$ centers was investigated with respect to the literature controversies concerning the identification of both signals with Carbon Vacancy. We demonstrate that such identification holds only in some cases and such we conclude that $Z_{1,2}$ and $EH_{6,7}$ signals cannot come from the same defect.

On Silicon: 1) All the GL diodes present an intrinsic holes trap having and activation energy of 0.27 eV, except for the GL diodes co-implanted with Carbon in the highest dose ($5x10^{14}$ $/cm^2$) where strongly disturbed spectra are recorded. Fig. 2 depicts the defects induced by 23 GeV protons in the different flavours of GL diodes and their characteristics; 2) On LGADs, we succeed corelating the defect investigations with the observed macroscopic damage. For example, the C implantation induce mid-gap energy level (MGL) responsible for the high leakage current and the slight decrease in the gain layer depletion voltage (Fig.3); 3) Elucidation of the chemical nature of X defect in low resistivity p-

type Si- a center with enhanced field emission. Contrary to the expected impact on N_{eff} the center proved unharmful. Therefore, in-depth investigations of the emission rate were performed. We demonstrate a phonon-assisted tunnelling mechanism for charge emission from the X defect, pointing out that it does not impact on N_{eff}. Furthermore, the measured characteristics of the X-Defect, including apparent activation energy, capture cross-section and emission mechanism points out to the identification with the donor state of the singly charged di-vacancy, $V_2(+/0)$.

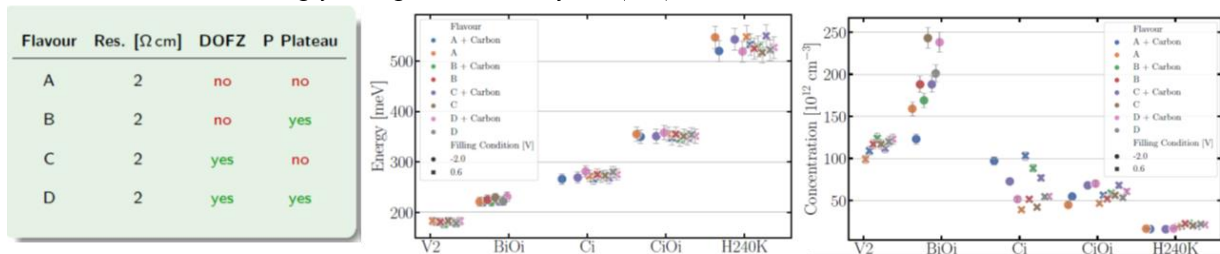

Flavour	Res. [Ω cm]	DOFZ	P Plateau
A	2	no	no
B	2	no	yes
C	2	yes	no
D	2	yes	yes

Figure 2. Results of DLTS investigations in GL diodes irradiated with $2x10^{14}$ protons (23 GeV)/cm^2.

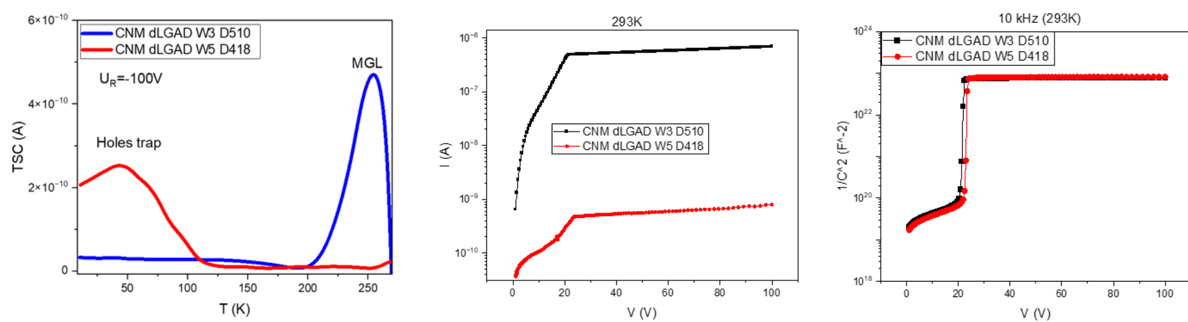

Figure 3. Results on p-type deep-LGADs. W3 sample is co-implanted with C and W5 is not.

The *MD simulations* have been performed on large Si supercells (10000 atoms). A group of 10 Si atoms are displaced from their initial crystallographic positions, by setting high initial kinetic energies. We visualize the process of V-I pair production and recombination by showing a few snapshots of the relevant phases in Fig. 4. The V and I migration is also evidenced. *Using DFT, we investigated boron related defects*, such as $B_{Si}Si_i$ and B_iO_i, which present donor-like character in p-type doping conditions. This behaviour is confirmed for $B_{Si}Si_i$ and, in the case of B_iO_i, besides the standard configuration, we identified another metastable state, with a different structural configuration, presenting Boron and Oxygen atoms in close proximity (see Fig. 5).

Figure 4. MD simulations of vacancy-interstitial pair production and recombination. V (grey) / I (magenta)

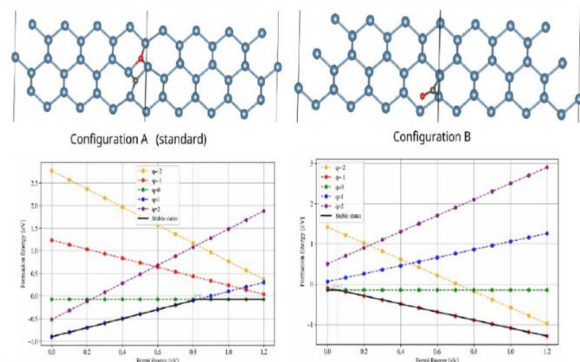

Figure 5. DFT simulations of B_iO_i defect in standard and metastable configuration.

The envisaged technological output is the knowledge-based radiation hard material design for particle detection Si and SiC based sensors.